Inorg. Chem. **2006**, *45*, 10807–10814

F/Cl-Exchange on $AlCl_3$−Pyridine Adducts: Synthesis and Characterization of *trans*-Difluoro-tetrakis-pyridine-aluminum-chloride, $[AlF_2(Py)_4]^+Cl^-$

Anton Dimitrov, Detlef Heidemann, and Erhard Kemnitz*

Institute of Chemistry, Humboldt University of Berlin, Brook-Taylor-Strasse 2, 12489 Berlin, Germany

Received August 8, 2006

Whereas liquid CCl_3F reacts with solid $AlCl_3$ exothermically under chlorine–fluorine-exchange already above −20 °C, no reaction takes place between CCl_3F and the pyridine complexes of $AlCl_3$ ($AlCl_3$·Py, $AlCl_3$·2Py, or $AlCl_3$·3Py) up to 100 °C. The desired chlorine by fluorine substitution on the monomer $AlCl_3$–pyridine adducts occurs, however, easily using Me_3SiF as fluorinating agent. By reacting $AlCl_3$·3Py with Me_3SiF (even up to 10-fold stoichiometric excess) in pyridine as a solvent, only two of the three Cl atoms can be substituted by fluorine, leading in good yield to the new "mixed aluminum halide", AlF_2Cl·4Py. Actually, it represents the first example of a stable solid donor–acceptor adduct of an aluminum-III halide with two different halogens of defined stoichiometry. It was characterized by multinuclear solid-state NMR (^{27}Al and ^{19}F), IR spectroscopy, as well as single-crystal structure analysis. The new compound has an ionic solid-state structure with helical *trans*-octahedral $[(Py)_4AlF_2]^+$ cations and isolated Cl^- anions. The comparison of its ^{27}Al MAS solid-state NMR spectra with those of a compound bearing the analogous $[(Py)_4AlCl_2]^+$ cation reveals an extreme increase in the quadrupolar coupling constants, from 0.24 MHz in case of the chlorine cation to about 16 MHz in case of the new $[(Py)_4AlF_2]^+$ cation.

1. Introduction

In the course of our research work concerning the development and synthesis of new heterogeneous metal fluorides-based catalysts, we are investigating some AlF_3 phases besides the known crystalline AlF_3 modifications. These are noncrystalline with respect to XRD but well defined and understood as solids.[1] ACF, a "chlorine containing" AlF_3 phase easily accessible by Cl/F-exchange with $AlCl_3$ (ACF: $AlCl_xF_{3-x}$, $x = 0.05-0.30$)[2−4] and "high surface" AlF_3 (HS-AlF_3)[5,6] obtainable by a two-step non-aqueous sol−gel method, represent the most prominent amorphous AlF_3 phases. They behave like very strong solid Lewis acids and, consequently, are able to catalyze the same reactions and are efficient as liquid SbF_5. To a lesser extent, both compounds can be partially dissolved in pyridine (Py), and only in ^{19}F NMR spectra of the ACF/Py solutions does a sharp signal appear at about −173 ppm. Similar signal positions (at about −175 ppm) were observed by Roesky at al.[7] in ^{19}F NMR spectra of donor acceptor complexes between difluoro-amido-alanes and tetrahydrofurane, $R^aR^bN-AlF_2$·THF, which according to X-ray single-crystal determination possess tetra-coordinated Al species and monomer molecular structures.[8] The crystal structures of two derivatives of $R^aR^bN-AlF_2$·THF with $R^a = 2,6\text{-}{}^iPr_2C_6H_3$ and $R^b =$ either $^iPr-SiMe_2$ or $^tBu-SiMe_2$ as well as of the monomeric $[(THF)_4AlF_2]^+$ cation[9] from the organometallic compound

* To whom correspondence should be addressed. E-mail: erhard.kemnitz@chemie.hu-berlin.de.

(1) Kemnitz, E.; Menz, D.-H. *Prog. Solid State Chem.* **1998**, *26*, 97−153.
(2) (a) Krespan, G. C.; Dixon, D. A. *J. Fluorine Chem.* **1996**, *77*, 117−126. (b) Krespan, G. C.; Petrov, V. A. *Chem. Rev.* **1996**, *96*, 3269−3301. (c) Petrov, V. A.; Krespan, G. C.; Smart, B. E. *J. Fluorine Chem.* **1996**, *77*, 139−142. (d) Petrov, V. A.; Krespan, G. C.; Smart, B. E. *J. Fluorine Chem.* **1998**, *89*, 125−130. (e) Petrov, V. A.; Krespan, G. C. *J. Fluorine Chem.* **2000**, *102*, 199−204.
(3) Krahl, Th.; Stösser, R.; Kemnitz, E.; Scholz, G.; Feist, M.; Silly, G.; Buzaré, J.-Y. *Inorg. Chem.* **2003**, *42*, 6474−6483.
(4) Krahl, Th.; Kemnitz, E. *J. Fluorine Chem.* **2006**, *127*, 663−678.
(5) Kemnitz, E.; Gross, U.; Rüdiger, St.; Shekar, S. Ch. *Angew. Chem., Int. Ed.* **2003**, *36*, 4251−4254.
(6) Rüdiger, St.; Gross, U.; Feist, M.; Prescott, H.; Shekar, S. Ch.; Troyanov, S.; Kemnitz, E. *J. Mater. Chem.* **2005**, *15*, 588−597.
(7) Waezsada, S.; Liu, F.-Q.; Murphy, E.; Roesky, H.; Teichert, M.; Uson, I.; Schmidt, H.-G.; Albers, Th.; Parisini, E.; Noltemeyer, M. *Organometallics* **1997**, *16*, 1260−1264.
(8) Waezsada, S.; Liu, F.-Q.; Barnes, C.; Roesky, H.; Montero, M.; Uson, I. *Angew. Chem., Int. Ed. Engl.* **1997**, *36*, 2625−26527.

10.1021/ic061493x CCC: $33.50
Published on Web 11/24/2006

$[(THF)_4AlF_2]^+[\{(SiMe_3)_3C\}_2Al_2F_5]^-$ are the only known three structural examples of a monomer "aluminum fluoride" till now having all of their F atoms in discrete terminal positions. The latter compound is stable only at low temperature and undergoes decomposition above 0 °C.[9]

The recordings of signals at −173 ppm in ^{19}F NMR spectra of ACF/Py solutions (analogous to the signals of R_2NAlF_2·THF) as well as the presence of Cl anions therein raised the question whether treatment of ACF by pyridine led to the formation of a discrete Al−F species (AlF_3·*n*Py, AlF_2Cl·*n*Py, $AlFCl_2$·*n*Py, $n \geq 1$). Although mixed aluminum chloride-fluorides ($AlCl_xF_{3-x}$, $x = 1-2$) have been theoretically investigated repeatedly,[10] the experimental proof for their existence was possible only by high-temperature mass spectrometric investigations of the $Al-AlF_3-AlCl_3$ system[11] and by IR spectroscopy in a matrix.[10] We agree with Roesky et al.[8] that the compound $[(Me_3C)_2SiNCMe_3]_2AlF_2Cl$ has incorrectly been discussed in the literature[12] as a room-temperature stable donor acceptor complex of AlF_2Cl; due to the determination of quite usual bond lengths for Si−F (170.8 pm) and Al−N (184.7 pm), this compound represents a bis-(diorganylamido)-chloroalane, $[(Me_3C)_2SiFNCMe_3]_2$-AlCl. Its discrete monomeric molecular structure in the solid state is stabilized by weak intramolecular interactions between the fluorine atoms of both organo-silicon substituents and aluminum with Al−F contacts of 208.5 pm. In addition to the above-mentioned reports,[8,9,12] there are no more examples given in the literature regarding structures bearing discrete Al−F bonds or representing a solid aluminum-chloride-fluoride (including polymer structures of AlF_2Cl or $AlFCl_2$). In contrast, more than 20 single-crystal structures of solid donor acceptor adducts of $AlCl_3$ have been published, hereunder a number of $AlCl_3$ adducts with unidentate nitrogen bases. Dependent on the stoichiometric composition of the complexes, coordination numbers of 4, 5, or 6 at the Al central atom have been determined by X-ray single-crystal analysis.[13−16]

From reactions of $AlCl_3$ with pyridine, the complexes $AlCl_3$·Py (**1**), $AlCl_3$·2Py (**2**), and $AlCl_3$·3Py (**3**) have been reported,[15,17] but only **2** and **3** were structurally characterized: **2** as the ionic species $[(Py)_4AlCl_2]^+[AlCl_4]^-$ and **3** as the nonionic octahedral complex $AlCl_3$·3Py. With our X-ray study of **1**, the missing structural information for all three synthesized $AlCl_3$·*n*Py ($n = 1-3$) complexes has been completed. Until our preliminary results, recently presented at the 18th International Symposium on Fluorine Chemistry,[18] no reactions attempting a Cl/F-exchange with $AlCl_3$ complexes had been reported. The reaction of $AlCl_3$·3Py (**4**) with Me_3SiF aimed at the synthesis of $[(Py)_4AlF_2]^+Cl^-$ (**4**), and a room-temperature stable complex with a monomer molecular structure in the solid state was obtained. The reaction details for the preparation of **4** as well as its characterization by multinuclear solid-state NMR (^{27}Al and ^{19}F), IR spectroscopy, and single-crystal XRD analysis are reported in this study.

2. Experimental Section

General. All experiments were performed under a purified dry inert gas atmosphere (argon) in a glove box and/or in a glass high-vacuum line. Solvents and pyridine were purified according to standard procedures and freshly distilled prior use. $AlCl_3$ (99.999%, Aldrich), $CFCl_3$ (99.5%, Fluka), and Me_3SiF (96%, Aldrich) were used without further pretreatment.

Methods. X-ray diffraction (XRD) measurements of powder samples were performed on a Seiffert RD7 (Freiberg, Germany) with Cu K_α (154.06 pm) radiation. The moisture-sensitive samples were prepared in a dry box, covered with a special X-ray amorphous polystyrene foil, and sealed with Kel-F grease (Roth).

Single-crystal XRD analysis was carried out on an IPDS diffractometer (Stoe & Cie) at 180 K using graphite-monochromated Mo K_α (71.073 pm) radiation and a cryostream cooler (Oxford Cryosystems). The moisture-sensitive samples were fixed on the tip of a glass needle in a cold stream of nitrogen. The structures were solved[19] and refined[20] with the SHELTL program suite.

FT-IR spectra of KBr pellets were recorded on a Perkin-Elmer 2000 spectrometer in transmission mode. About 400 mg of KBr (for optical properties, Fluka) was pressed with 1.5−2.0 mg of the sample inside the dry box, and then measured in the regions 4000−400 cm^{-1}.

Solid-state NMR spectra were recorded at room temperature on a Bruker Avance 400 spectrometer, operating at frequencies of 104.3 MHz for ^{27}Al and 376.4 MHz for ^{19}F.

The MAS NMR measurements were performed using a 4 mm and a 2.5 mm double-bearing double tuned ($^1H/^{19}F$-X) MAS probe (Bruker Biospin) at spinning rates between 12 and 15 kHz and between 25 and 30 kHz, respectively.

The ^{27}Al MAS spectra were obtained using single pulse excitation with pulse durations of 1 μs ($\pi/12$ pulses) ensuring a linear irradiation regime and minimizing the distortion of the spectra. To obtain a reliable signal-to-noise ratio, the spectra of the fluorine-free samples were recorded by accumulating up to 512 scans with a recycle delay of 5 s, and the spectra of the fluorine-containing sample were recorded by accumulating up to 72 800 scans with a recycle delay of 1 s.

Up to 16 K data sampling points were recorded over a maximum 1 MHz spectrum width.

Processing of the free induction decay was realized using the Bruker XWINNMR software. The first points (up to 20) corrupted by electronic interferences were removed, and an equal number, augmented of the points lost during the dead time previous

(9) Hatop, H.; Roesky, H.; Laban, Th.; Röpken, C.; Sheldrick, G.; Bhattacharjee, M. *Organometallics* **1998**, *17*, 4326−4328.
(10) Himmel, H.-J.; Bahlo, J.; Haussmann, M.; Kurth, F.; Stösser, G.; Schnöckel, H.-G. *Inorg. Chem.* **2002**, *41*, 4952−4960.
(11) Farber, M.; Harris, S. P. *High Temp. Sci.* **1971**, *3*, 231.
(12) Clegg, W.; Klingebiel, U.; Neemann, J.; Sheldrick, G. M. *J. Organomet. Chem.* **1983**, *249*, 47−54.
(13) Grant, D. F.; Killean, R. C. G.; Lawrence, J. L. *Acta Crystallogr.* **1969**, *B25*, 377−379.
(14) Ahmed, A.; Schwarz, W.; Weidlein, J.; Hess, H. *Z. Anorg. Allg. Chem.* **1977**, *434*, 207−216.
(15) Pullmann, P.; Hensen, K.; Bats, J. *Z. Naturforsch.* **1984**, *37b*, 1312−1315.
(16) Engelhardt, L. M.; Junk, P. C.; Raston, C. L.; Skelton, B. W.; White, A. H. *J. Chem. Soc., Dalton Trans.* **1996**, 3297−3301.
(17) (a) Wilson, J. W.; Worrall, I. J. *Inorg. Nucl. Chem. Lett.* **1967**, *3*, 57−60. (b) Wilson, J. W.; Worrall, I. J. *J. Chem. Soc. A* **1968**, 316−317.
(18) Dimitrov, A.; Heidemann, D.; Kemnitz, E. *Abstracts*, 18th ISFC, Bremen (Germany), 2006; p 80.
(19) Sheldrick, G. M. *Acta Crystallogr.* **1990**, *A46*, 467−473, aus dem Programm SHELXS.
(20) Sheldrick, G. M. *SHELXL-97, Program for Crystal Structure Refinement*; Göttingen, 1997.

Table 1. Crystal Structure Information for $AlCl_3$·Py (**1**), $[(Py)_4AlF_2]Cl$ (**4**), and $[(Py)_4AlF_2]Cl$·2[PyH]Cl (**5**)

	compound		
	1	**4**	**5**
formula	$C_5H_5AlCl_3N$	$C_{20}H_{20}AlClF_2N_4$	$C_{30}H_{32}AlCl_3F_2N_6$
Fw (g/mol)	212.43	416.83	647.95
crystal system	monoclinic	monoclinic	orthorhombic
space group (no.)	$P2_1/n$ (14)	$C2/c$ (15)	$Pccn$ (56)
crystal size/mm	0.64; 0.54; 0.42	0.30; 0.26; 0.24	0.32; 0.30; 0.28
a/Å	6.382(1)	14.706(1)	12.411(2)
b/Å	15.921(3)	11.529(1)	13.135(2)
c/Å	9.192(2)	12.985(1)	21.952(3)
β/deg	102.91(2)	118.04(1)	90.00
V/Å^3	910.4(3)	1943.3(3)	3579.8(8)
ρ_{calc}/g cm^{-3}	1.550	1.425	1.202
Z	4	4	4
μ(Mo Kα)/mm^{-1}	1.030	0.274	0.318
2Θ − range/deg	6.8−52.2	7.0−66.0	4.9−50.1
no. of reflns (total/indep)	6235/1766	10 314/3701	20 661/3171
R_{int}	0.0723	0.0385	0.1049
reflns, $I > 2\sigma(I)$	1509	3088	2068
reflections/params	1766/96	3701/139	3171/208
R1[a] [$F_0 > 4\sigma(F_0)$]	0.0347	0.0396	0.0452
wR2[b] (all data)	0.0941	0.0907	0.0987
GOF (all data)	1.071	1.068	0.881
ρ_{final} (max/min)/e Å^{-3}	0.332/−0.432	0.491/−0.495	0.437/−0.177

[a] $R1 = \sum||F_o| - |F_c||/\sum|F_o|$. [b] $wR2 = [\sum w(F_o^2 - F_c^2)^2/\sum w(F_o^2)^2]^{1/2}$.

acquisition, were reconstructed by using the backward linear prediction method.

The ^{19}F MAS spectra were obtained using single pulse excitation consisting of 2 μs pulses ($\pi/2$ pulses) and recycle delays of 10 and 60 s to exclude saturation effects. Up to 128 FIDs were accumulated to obtain a reliable signal-to-noise ratio. In addition to the above-mentioned single pulse sequence, a phase-cycled depth pulse sequence according to Cory and Ritchey[21] was applied to suppress the strong background signal from the probe head.

Up to 2 K data sampling points were recorded over a maximum 400 kHz spectrum width.

The ^{27}Al and ^{19}F spectra were externally referenced to 1 M aqueous $AlCl_3$ solution and to liquid $CFCl_3$ at 0 ppm, respectively.

The NMR parameters (chemical shifts, line widths, quadrupolar coupling constants) were fitted to the experimental spectra using the Topspin software (Bruker Biospin) and the dmfit[22] software package.

Sample Preparation. ACF (ACF: $AlCl_xF_{3-x}$, $x = 0.05-0.30$) was prepared from $AlCl_3$ and $CFCl_3$ according to the procedure described in the literature.[2−4]

$AlCl_3$·Py, $AlCl_3$·2Py, or $AlCl_3$·3Py (1−3). 1−3 have been prepared from reactions of $AlCl_3$ with the corresponding stoichiometric amounts of pyridine using benzene as a solvent. The purity of each compound was confirmed by complete elemental analysis, powder XRD, and ^{27}Al solid-state NMR. Single crystals of **1** suitable for X-ray structure determination were grown in toluene at −30 °C. Our structural investigations of **2** and **3** confirmed the information from the literature.[14] The single-crystal data obtained were transformed by DIAMOND[23] to the corresponding powder patterns and used for checking the purity of the bulk samples by XRD prior to recording the ^{27}Al MAS NMR spectra. The corresponding ^{27}Al MAS NMR spectroscopical data are summarized in Table 3.

(21) Cory, D. G.; Ritchey, W. M. *J. Magn. Reson.* **1988**, *80*, 128−132.
(22) Massiot, D.; Fayon, F.; Capron, M.; King, I.; Le Calvé, S.; Alonso, B.; Durand, J. O.; Bujoli, B.; Gan, Z.; Hoatson, G. *Magn. Reson. Chem.* **2002**, *40*, 70−76.
(23) Brandenburg, K.; Berndt, M. *Diamond 2.1c*; Crystal Impact GbR: Bonn, Germany, 1999.

Table 2. Selected Bond Lengths (pm) and Angles (deg) for $[(Py)_4AlF_2]^+Cl^-$ (**4**) and $[(Py)_4AlF_2]^+$·2[PyH]$^+$·3Cl$^-$ (**5**)

compound	Al−F	Al−N1	Al−N2	F−Al−N1	F−Al−N2	N1−Al−N2
4	171.94(6)	206.83(9)	207.69(9)	90.37(3)	90.09(3)	92.63(3)
5	172.5(1)	206.0(2)	207.2(2)	89.94(7)	89.97(7)	90.83(8)

Table 3. Results of the ^{27}Al MAS NMR Studies

sample	C.N.[a]	δ[b] [ppm]	QCC[c] [kHz]	η[d]
(**1**) $AlCl_3$·1Py	4	103.1	1175[f]	0.4[f]
(**2**) $AlCl_3$·2Py				
$[AlCl_4]^-$	4	101.4	750[f]	1[f]
$[AlCl_2$·4Py$]^+$	6	24.6	241[e]	0.49[e]
(**3**) $AlCl_3$·3Py	6	20.4	847[f]	0.4[f]
(**4**) AlF_2Cl·4Py				
$[Cl]^-$				
$[AlF_2$·4Py$]^+$	6	3.6[e]	16 070[e]	0.08[e]
$AlCl_3$	6	−1.4	455[e]	0.34[e]

[a] C.N., coordination number of the aluminum atom under study. [b] δ, isotropic ^{27}Al chemical shift. [c] QCC, quadrupole coupling constant ($=e^2qQ/h$) as a function of the electric quadrupole moment eQ, the z-component, $V_{zz} = eq$, of the electric field gradient tensor, and Planck's constant, h.[d] η, asymmetry parameter ($=(V_{xx} - V_{yy})/V_{zz}$) as a function of the x, y, and z components of the electric field gradient (EFG) tensor. [e] Calculated value. [f] Estimated value.

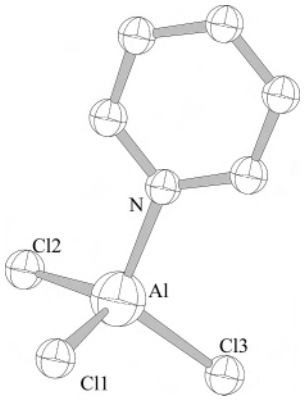

Figure 1. Crystal structure of $AlCl_3$·Py (**1**) (DIAMOND,[23] the ellipsoids represent a 50% probability; for clarity, H-atoms are not shown, C-atoms are not labeled). Selected bond lengths [pm]: Al(1)−Cl(1) 212.36(9), Al(1)−Cl(2) 212.61(9), Al(1)−Cl(3) 211.65(9), Al(1)−N(1) 193.0(2).

$[(Py)_4AlF_2]^+Cl^-$ (4). Compound **3** (3.71 g, 10.0 mmol) was partially dissolved in pyridine (50 mL) in a 150 mL Schlenk tube. To this suspension was added 3 equiv of Me_3SiF at −20 °C within 2 h. After the mixture was stirred additionally for 2 h at room temperature, the reaction was complete, and the Me_3SiF excess was removed by pumping off. The formed precipitate as a bright fine crystalline solid was filtered and recrystallized from hot pyridine. The resultant colorless needle-shaped crystals of compound **4** were separated, washed with pyridine, and dried in vacuo at room temperature. Yield: 3.04 g (72.5%). Anal. Calcd for $C_{20}H_{20}N_4AlF_2Cl$ (MW 416.83): C, 57.35; H, 4.81; N, 13.37; Al, 6.44; F, 9.54; Cl, 8.46. Found: C, 56.65; H, 4.91; N, 13.03; Al, 6.32; F, 9.31; Cl, 8.73. NMR spectroscopic data: ^{19}F NMR (Py-d_5), δ −173; ^{19}F MAS NMR, δ −170.3; ^{27}Al MAS NMR (data in Table 1 and Figure 2). IR spectra (KBr, cm^{-1}): 3059, 1608, 1537, 1485, 1447, 1216, 1150, 1072, 1062, 1047, 1017, 883, 767, 698, 641, 446.

$[(Py)_4AlF_2]^+$·2[PyH]$^+$·3Cl$^-$ (5). An accidental diffusion of moisture into the pyridine solutions of compound **4** induced the precipitation of unidentified hydrolysis products and, occasionally, the formation of colorless block-shaped crystals identified by single-crystal X-ray analysis as compound **5**.

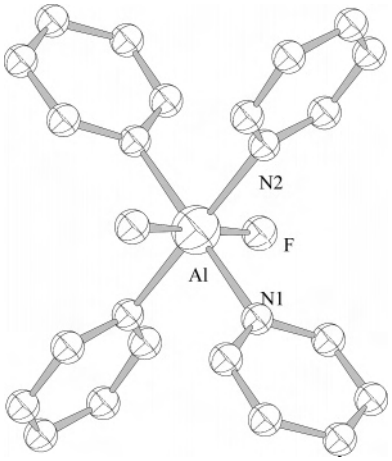

Figure 2. Structure of the cationic part of $[(Py)_4AlF_2]^+Cl^-$ (**4**) (DIAMOND,[23] the ellipsoids represent a 60% probability; for clarity, H-atoms are not shown, C-atoms and atoms created by symmetry are not labeled).

Crystallographic data (excluding structure factors) for the structures reported in this paper have been deposited with the Cambridge Crystallographic Data Centre as supplementary publications no. CCDC-623843 for **1**, no. CCDC-623844 for **4**, and CCDC-623845 for **5**. Copies of the data can be obtained free of charge on application to CCDC, e-mail: deposit@ccdc.cam.ac.uk.

3. Results

General. As compared to the preparation[2] of ACF by reacting solid $AlCl_3$ with liquid CCl_3F above −20 °C, no equivalent Cl/F-exchange reactions of compounds **1**−**3** with CCl_3F were observed up to 100 °C. By ^{27}Al and ^{19}F NMR solid-state spectra, recorded after heating of **1**−**3** with CCl_3F for several hours, it was shown that neither in toluene as a solvent nor in ampule-experiments without a solvent does Al−F bond formation take place. Instead, evolution of pyridine from **3** and **2** at higher temperature resulting in the formation of **2** and/or **1** was observed. However, the desired Cl/F-exchange takes place easily by reacting compounds **1**−**3** with Me_3SiF. Particularly, the fluorination of compound **3** with Me_3SiF in pyridine as a solvent leads to the selective formation of the new title compound **4** in good yields.

$$\underset{\mathbf{3}}{AlCl_3\cdot 3C_6H_5N} + 2Me_3SiF + n\mathrm{Py} \rightarrow \underset{\mathbf{4}}{AlF_2Cl\cdot 4C_6H_5N} + 2Me_3SiCl + (n-1)\mathrm{Py} \quad (1)$$

Obviously, the Lewis acidity of AlX_3 is increasing by the progressive substitution of Cl by F in the course of the halogen exchange reaction. At the particular fluorination stage after the substitution of two Cl-atoms, ongoing from $AlCl_3\cdot 3C_6H_5N$ to $AlF_2Cl\cdot 3C_6H_5N$, the necessary increase of the Lewis acidity value has been possibly reached, so that the reaction according to eq 2 becomes favorable as compared to the F/Cl-exchange reaction, resulting in the substitution of the last Cl-ligand of the first coordination sphere of the Al-complex by Py. Thus, reacting the molecular complex $AlCl_3\cdot 3Py$ with up to 10-fold stoichiometric excess of Me_3SiF in pyridine as a solvent (eq 1), only two of the three primary Cl-atoms can be substituted by fluorine,

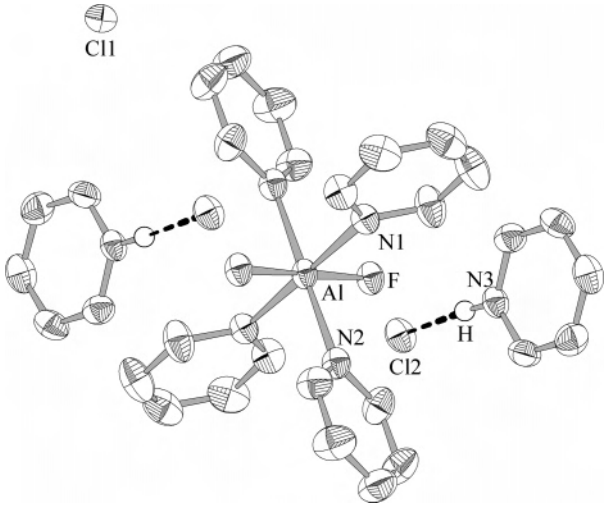

Figure 3. Crystal structure of $[(Py)_4AlF_2]^+\cdot 2[PyH]^+\cdot 3Cl^-$ (**5**) (DIAMOND,[23] the ellipsoids represent a 50% probability; C-atoms and atoms created by symmetry are not labeled). For clarity, all H-atoms are omitted, except the two forming both pyridinium cations and mediating H-bonds between N(3) and Cl(2): $d_{N(3)-Cl(2)} = 298.3(3)$ pm; $-_{N(3)-(H)-Cl(2)} = 173(2)°$.

resulting in good yield of the new donor−acceptor complex $AlF_2Cl\cdot 4Py$ (**4**). Formation of the corresponding ionic chloro complex by reacting **3** with Py (cf., eq 3) was not observed.

$$AlF_2Cl\cdot 3C_6H_5N + n\mathrm{Py} \rightarrow [(C_6H_5N)_4AlF_2]^+Cl^- + (n-1)\mathrm{Py} \quad (2)$$

$$AlCl_3\cdot 3C_6H_5N + n\mathrm{Py} \not\rightarrow [(C_6H_5N)_4AlCl_2]^+Cl^- \quad (3)$$

Structural Description. Crystallographic data for the three new compounds **1**, **4**, and **5** are summarized in Table 1; selected bond lengths and angles for **4** and **5** are in Table 2. The molecular geometry of **1** determined from the single-crystal structure analysis is shown in Figure 1. The aluminum, as expected, is in a distorted tetrahedral arrangement. No significant intermolecular short contacts were detected between the discrete monomer molecular buildings blocks of the crystal. The mean Al−Cl bond of about 212 pm is typical for Cl compounds of four-coordinated aluminum comparable to the bond distances found in the $[AlCl_4]^-$ anion of **2**.[15] The detected Al−N coordination distance of 193.0 pm is similar to those observed in the corresponding 1:1 adducts of $AlCl_3$, with trimethylamine (196.0 pm),[13] 2-methylpiridine (194.2 pm),[16] 2-diphenylmethylpyridine (195.4),[16] or quinoline (195.9 pm).[16]

The measured bond lengths and angles in $[(Py)_4AlF_2]^+$ cations of **4** and **5** are nearly identical (Table 2), and, consequently, the following discussion on compound **4** (Figure 2) applies fully to compound **5** (Figure 3), too. The structure of **4**, shown in Figure 2, reveals that the stabilization of the cationic fragment AlF_2^+ occurs easily by four molecules of pyridine in the same manner as it stabilizes the cationic part $AlCl_2^+$ of compound **2**; in all cases, the stable $[(Py)_4AlX_2]^+$ octahedron is formed. The Al−N-coordination bond distances in **2** (206.3 and 207.7 pm)[15] and **4** (206.8 and 207.7 pm) do not differ from each other, demonstrating that the large shortening of the Al−X bonds

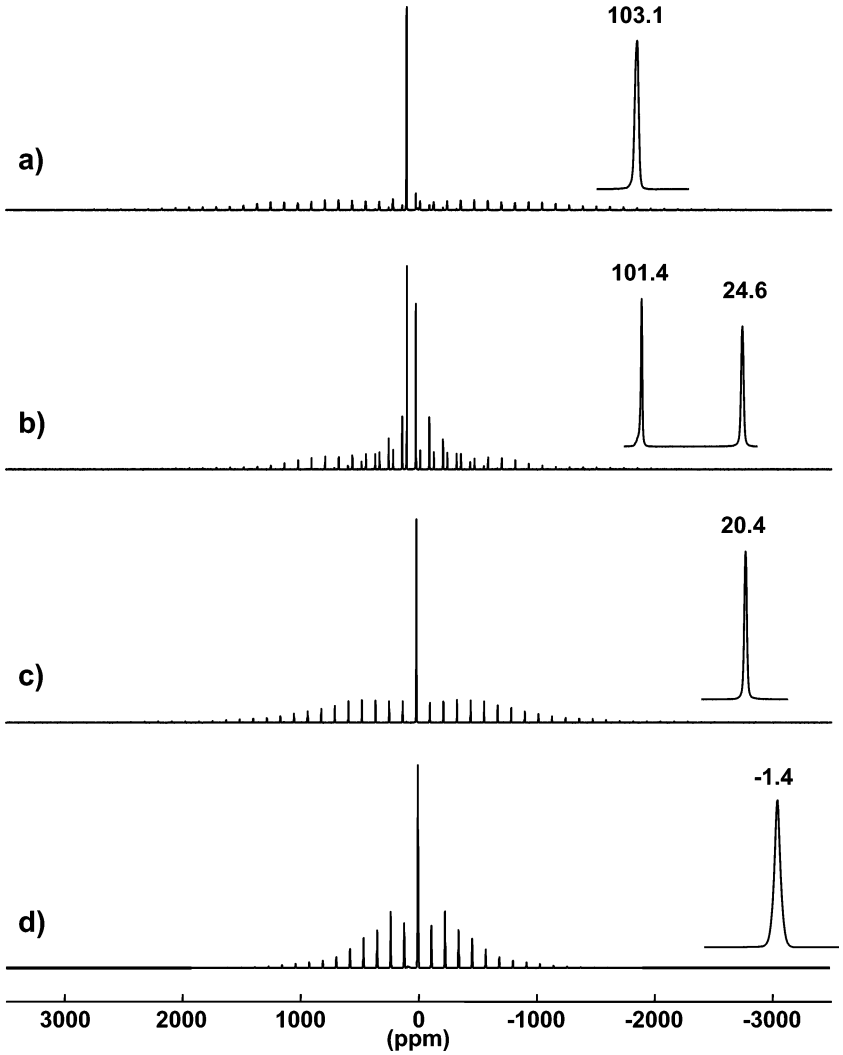

Figure 4. ^{27}Al MAS NMR spectra of $AlCl_3$·Py **1** (a), $AlCl_3$·2Py **2** (b), $AlCl_3$·3Py **3** (c), and $AlCl_3$ (d) measured with 12 kHz spinning frequency (the central transitions of the resonance signals with the respective values of the ^{27}Al chemical shifts are shown as insets).

on going from Cl to F is not influencing the strength of the Al−N donor−acceptor bonds at all. Furthermore, by comparing the cationic species within the structures of compounds **2** and **4** with the nonionic octahedral structure of **3** (Al−N bond distances: 206.7, 207.5, and 209.6 pm),[15] it was shown that the positive electrical charge does not significantly influence the corresponding Al−N distances, too. The Al−F distances in **4** and **5** are comparable to the Al−F bond lengths determined by Roesky et al.[9] in the $[(THF)_4AlF_2]^+$ cation and are within the shortest Al−F bond distances determined to date in compounds of six-coordinated aluminum.

NMR Investigation. In the syntheses of this study, ^{27}Al and ^{19}F MAS NMR spectroscopy was used as an analytical tool to characterize the samples obtained by different approaches and to optimize the preparation routes for the pure compounds reported in this paper. In a second step, the well-characterized crystalline samples were studied by means of ^{27}Al and ^{19}F MAS NMR measurements to derive correlations between parameters of the NMR spectra and the X-ray crystal structures. Such correlations will be useful for the interpretation of NMR spectra of amorphous $AlCl_3-AlF_3$-containing phases.

The spectra of the ^{27}Al MAS NMR studies of the fluorine-free compounds obtained with a spinning speed of 12 kHz are summarized in Figure 4. The corresponding spectrum of $AlCl_3$ is included for comparison (Figure 4d).

The presented ^{27}Al MAS MNR spectra are typical first-order quadrupolar spectra containing one (compounds **1**, **3**, and $AlCl_3$) or two (compound **2**) sharp resonance signals of nearly Gaussian line shapes due to the central transition and a set of spinning sidebands caused by the satellite transitions of the aluminum nuclei. The spectra of the individual compounds differ in the value of the chemical shift as well as the number and the intensity distribution of the spinning sidebands.

The chemical shift values reflect the details of the crystal structures of the studied samples. The single resonance signals obtained for **1**, **3**, and $AlCl_3$ are consistent with the single crystallographic sites of the aluminum in these structures, and the two signals for sample **2** reflect the existence of two different aluminum sites in agreement with the ionic structure determined by XRD analysis. The

measured chemical shifts between −1.4 and 24.6 ppm for $AlCl_3$, **3**, and **2**, all of them with octahedrally coordinated aluminum, are in the well-established chemical shift region for hexa-coordinated aluminum.[24,25] The measured chemical shifts of 103.1 and 101.4 ppm for the tetrahedrally coordinated aluminum in **1** and **2** are more high-frequency shifted as compared to the chemical shift region of tetrahedrally coordinated aluminum containing oxygen in the first coordination shell.[25] Because not only the atoms of the first coordination sphere contribute to the chemical shift of the aluminum but also other factors, like the local geometry, there is no conclusive explanation for this experimental results up to now. On the other hand, the measured ^{27}Al chemical shifts for aluminum environments containing both chlorine and pyridine in the first coordination sphere show a general trend. For the hexa-coordinated aluminum, the ^{27}Al shift moves from −1.4 ppm of "pyridine-free" $AlCl_3$ over 20.4 ppm for ($AlCl_3Py_3$) toward 24.6 ppm for $[AlCl_2Py_4]^+$. For tetrahedrally coordinated aluminum, the ^{27}Al chemical shift moves from 101.4 ppm for $[AlCl_4]^-$ anion of **2** to 103.1 ppm in **1** ($AlCl_3Py$). A formal substitution of chlorine by pyridine in the first coordination sphere of aluminum leads to a high-frequency shift of the ^{27}Al chemical shift or, in other words, to a lower shielding ("deshielding") of the aluminum nucleus. The unequal Al−Cl and Al−N bond lengths are inducing a larger electric field gradient around the Al nucleus in **1** than at the Al nucleus centered in the $[AlCl_4]^-$ part of **2** and, consequently, are responsible for the increase in QCC values of **1** as estimated from ^{27}Al NMR spectra (Table 3).

The spectra of the octahedrally coordinated aluminum in $AlCl_3$ and in $[AlCl_2Py_4]^+$ allowed the exact calculation of the quadrupolar coupling constants (QCC) and the asymmetry parameter of the electric field gradient (η) by simulating the manifold of the spinning sidebands. For the remaining spectra, the measured intensity distribution between the main signal and the spinning sidebands could not be simulated exactly so that only a raw estimation for QCC and η was possible in these cases. All obtained QCC and η are summarized together with the measured chemical shift values in Table 3.

A correlation of the QCC and η with details of the structure of the studied compounds could not be established.

In Figure 5, the sub-spectrum for the octahedrally coordinated aluminum in $[AlCl_2Py_4]^+$ obtained by simulation from the measured spectrum of sample **2** (see Figure 4b) is compared with the ^{27}Al MAS NMR spectrum of fluorine-containing sample $AlF_2Cl{\cdot}4Py$ (sample **4**) obtained at a spinning rate of 12 kHz. Although in both cases the aluminum atom is 6-fold coordinated by four pyridines and two halogens, the corresponding ^{27}Al MAS NMR spectra are totally different. On the first view, the ^{27}Al MAS NMR spectrum of sample **4** seemed to consist of several resonance signals with different line shapes due to second-order quadrupolar interaction. The variation of the spinning speed in a range up to 15 kHz resulted in similar spectra and gave no contribution to the interpretation of this spectrum. It was impossible to derive any useful information, neither about the chemical shift nor about the quadrupolar interaction and the EFG tensor. The application of higher spinning speeds by using a 2.5 mm MAS probe led to the solution of this problem. Above spinning rates of 25 kHz, the spectrum was clearly dominated by a single resonance signal with a typical line shape due to second-order quadrupolar interaction. The ^{27}Al MAS NMR spectrum of sample **4** obtained at a spinning rate of 30 kHz is shown in Figure 6a. A line shape simulation of the central transition without spinning sidebands in an enlarged scale (b) and including the corresponding spinning sidebands (c) as well as the simulation of both the central and the satellite transitions with all spinning sidebands (d) demonstrates the high accuracy of the analysis. The small signal at about −7 ppm marked with an asterisk (*) could be assigned to a hydrolysis product of the sample. The performed line shape simulation resulted in a chemical shift value of 3.6 ppm, a quadrupole coupling constant of about 16 MHz, and a η value of 0.08 (see Table 3). While the chemical shift of 3.6 ppm is in the usual range for octahedrally coordinated aluminum atoms, the QCC of 16.07 MHz is an extremely high value for quadrupole coupling constants and, by our knowledge, the largest ever measured for octahedral aluminum environments containing fluorine in the first coordination sphere. This extremely large QCC is the reason for the unusual line shape obtained at a spinning rate of 12 kHz. It should be pointed out that a line shape simulation using the data obtained from the high-speed MAS experiment considering a spinning rate of 12 kHz reproduces exactly the line shape of the measured spectrum in Figure 5b.

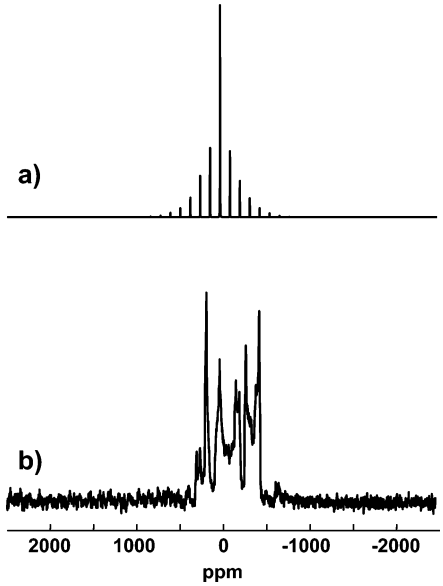

Figure 5. Experimental ^{27}Al MAS NMR spectra of the cationic species $[AlX_2Py_4]^+$, (a) X = Cl and (b) X = F, measured with a spinning rate of 12 kHz.

An analysis of the crystallographic data of both cations $[AlCl_2Py_4]^+$ and $[AlF_2Py_4]^+$ shows that the largest difference

(24) Müller, D.; Bentrup, U. *Z. Anorg. Allg. Chem.* **1989**, *575*, 17−25.
(25) Freude, D. Quadrupolar Nuclei in Solid-state Nuclear Magnetic Resonance. In *Encyclopedia of Analytical Chemistry*; Meyers, R. A., Ed.; John Wiley & Sons Ltd.: Chichester, 2000; pp 12188−12224.

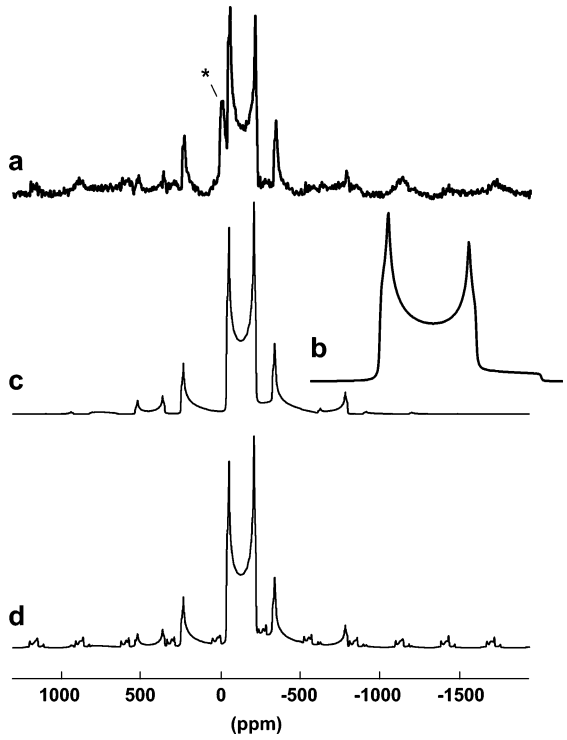

Figure 6. ^{27}Al MAS NMR spectrum of $[(Py)_4AlF_2]^+Cl^-$ (**4**) measured with a spinning rate of 30 kHz: (a) experimental spectrum, (b) simulated central transition without spinning sidebands (enlarged scale), (c) simulated central transition with spinning sidebands, and (d) simulated central and satellite transitions with corresponding spinning sidebands (*denotes the resonance signal of an impurity due to hydrolysis).

between the chlorine and the fluorine containing species is in the bond lengths of the aluminum−halogen bonds. In $[AlCl_2Py_4]^+$, a mean Al−Cl bond length of 228.5 pm was determined, whereas in $[AlF_2Py_4]^+$, the corresponding mean Al−F bond length is clearly shorter. A value of 171.9 pm was determined. The averaged Al−N bond lengths of 207.2 pm are equal in both cations and of the same order of magnitude as the Al−N bond distances determined from the nonionic octahedral structure of **3** (206.7, 207.5, and 209.6 pm).[15] The extreme decrease of the aluminum halogen distances on substitution of Cl by F with practically constant Al−N donor bond lengths led to the obvious changes in the geometries of the two cations and so in their symmetries: from distorted-(D_{4h}-elongated)-octahedron in case of $[AlCl_2Py_4]^+$ to distorted-(D_{4h}-compressed)-O_h-symmetry in case of $[AlF_2Py_4]^+$. The changes in the geometries of the aluminum species together with the increasing electronegativity of the F-ligands seem to be the main reasons for the very large electric field gradient in case of $[AlF_2Py_4]^+$. Consequently, its interaction with the electric quadrupole moment of the Al nucleus induces the large value of the QCC.

The ^{19}F MAS NMR spectra of $AlF_2Cl{\cdot}4Py$ obtained at spinning rates of 12 and 27 kHz are summarized in Figure 7. In both cases, a single signal with an isotropic chemical shift value of −170.2 ppm and a set of spinning sidebands that are due to residual dipolar interaction and chemical shift anisotropy are shown. By dissolving compound **4** in pyridine, this signal is slightly shifted to low frequency, and we

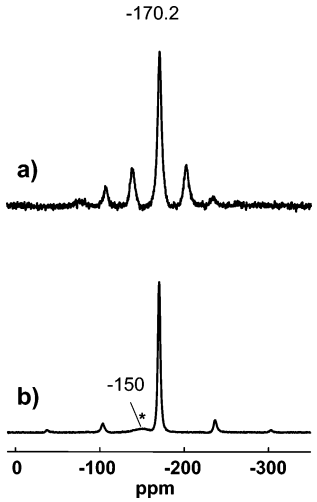

Figure 7. ^{19}F MAS NMR spectra of $AlF_2Cl{\cdot}4Py$ obtained at spinning rates of 12 kHz (a) and 27 kHz (b) (*denotes the resonance signal of an impurity due to hydrolysis).

observed a singlet at −173 ppm. The observation of a single signal in the ^{19}F MAS NMR spectra of $AlF_2Cl{\cdot}4Py$ reflects the existence of only one single fluorine site, in agreement with the XRD analysis. The measured chemical shift is within the typical range observed for F-atoms placed in the first coordination sphere of hexa-coordinated aluminum species. It is very close to the values detected for all crystalline modifications of AlF_3; for example, a value of −172.5 ppm has been detected for α-AlF_3, the most stable AlF_3 modification that has a polymer solid-state structure. At the higher spinning rate, a small signal at about −150 ppm is detectable, which has been assigned to the same hydrolysis product of the sample causing the ^{27}Al signal at ca. −7 ppm as we already mentioned by discussing the ^{27}Al MAS NMR spectra of compound **4**.

4. Conclusions

By solid-state X-ray study of $AlCl_3{\cdot}Py$, the missing structural information for all three synthesized $AlCl_3{\cdot}n$Py (n = 1−3) complexes has been completed.

Fluorination studies on the 1:3 $AlCl_3$−pyridine complex were aimed at the successful synthesis of $AlF_2Cl{\cdot}4Py$ by using Me_3SiF as fluorinating agent.

Lewis acidity of AlX_3 increases on substitution of Cl by F, making the substitution of chlorine by pyridine in the first coordination sphere of the difluoro-aluminum-species possible, and, hence, using pyridine as a solvent avoids the complete substitution of all chlorines by fluorine of $AlCl_3{\cdot}3Py$.

The new compound has an ionic solid-state structure with helical *trans*-octahedron $[AlF_2(C_6H_5N)_4]^+$ cations and isolated Cl^- anions.

All well-characterized crystalline samples were studied by means of ^{27}Al and ^{19}F MAS NMR measurements to derive correlations between parameters of the NMR spectra and details of the crystal structures required for the interpretation of NMR spectra of amorphous $AlCl_3$−AlF_3-containing samples. A formal substitution of chlorine by pyridine in

the first coordination sphere of aluminum leads to a lower shielding of the aluminum nucleus under study.

The ^{27}Al MAS NMR spectrum of $AlF_2Cl \cdot 4Py$ reveals unexpected complexity due to the very large QCC and can be resolved sufficiently only at spinning rates above 25 kHz. The extremely large value of the QCC is caused by an extreme shortening of the aluminum−halogen distances occurring during the substitution of Cl by F.

Acknowledgment. This Article is dedicated to Prof. Dr. Neil Bartlett on the occasion of his 75th birthday. We thank the EU for support of part of this work through the sixth Framework Programme (FUNFLUOS, Contract No. NMP3-CT-2004-5005575). We also thank Ms. Irmgard Hartwich for excellent technical assistance and Prof. S. I. Troyanov for discussion of structural details.

Note Added after ASAP Publication. This article was released ASAP on November 24, 2006 with a minor error in Figure 3. The correct version was posted on December 8, 2006.

IC061493X